Exploring Sulfur Chemistry in TMC-1 with NSRT

Exploring Sulfur Chemistry in TMC-1 with NSRT

Wasim Iqbal[1,2*], Xiaohu Li[1,2,3*], Juan Tuo[1,4], Ryszard Szczerba[1,2,5], Yanan Feng[1,4], Zhenzhen Miao[1,2], Jiangchao Yang[1,4], Jixing Ge[1,2], Gleb Fedoseev[1,2,6], Donghui Quan[7,1], Qiang Chang[8], Chuan-Lu Yang[1,9], Tao Yang[1,10], Gao-Lei Hou[11], Yong Zhang[1,12,13], Xuan Fang[1,14,13], Xia Zhang[1,2], Fangfang Li[1,2,4], Rong Ma[1,4], Xiaomin Song[1,4], Zhiping Kou[1,4], and Yuxuan Sun[1,4]

[1]*Xinjiang Astronomical Observatory, Chinese Academy of Sciences, Urumqi 830011, China*
[2]*Xinjiang Key Laboratory of Radio Astrophysics, Urumqi 830011, China*
[3]*Key Laboratory of Radio Astronomy, Chinese Academy of Sciences, Nanjing 210008, China*
[4]*University of Chinese Academy of Sciences, Beijing 100049, China*
[5]*Nicolaus Copernicus Astronomical Center, Rabiańska 8, 87-100 Toruń, Poland*
[6]*Research Laboratory for Astrochemistry, Ural Federal University, Kuibysheva St. 48, 620026 Ekaterinburg, Russia*
[7]*Astronomical Computing Research Center, Zhejiang Laboratory, Hangzhou 311100, China*
[8]*School of Physics and Optoelectronic Engineering, Shandong University of Technology, Zibo 255000, China*
[9]*School of Physics and Optoelectronic Engineering, Ludong University, Yantai 264025, China*
[10]*State Key Laboratory of Precision Spectroscopy, East China Normal University, Shanghai 200062, China*
[11]*MOE Key Laboratory for Non-Equilibrium Synthesis and Modulation of Condensed Matter, School of Physics, Xi'an Jiaotong University, Xi'an 710049, China*
[12]*School of Physics and Astronomy, Sun Yat-sen University, Guangzhou 510275, China*
[13]*Laboratory for Space Research, Faculty of Science, The University of Hong Kong, Hong Kong, China*
[14]*National Astronomical Observatories, Chinese Academy of Sciences, Beijing 100012, China*

(Received 5 November 2023; accepted manuscript online 21 December 2023)

There have been several studies on sulfur depletion in dense cores like TMC-1 (Taurus Molecular Cloud 1), employing updated reaction networks for sulfur species to explain the missing sulfur in the gas within dense clouds. Most of these studies used a C/O ratio of 0.7 or lower. We present NSRT (NanShan 26m Radio Telescope) observations of TMC-1 alongside results from time-dependent chemical simulations using an updated chemical network. Our findings highlight the impact of the C/O ratio on the gas-phase evolution of C_2S and C_3S. The simulation results show that the C/O ratio is an important parameter, playing a fundamental role in determining the gas-phase abundances of sulfur species in dense cores.

DOI: 10.1088/0256-307X/41/2/029501

It is crucial to estimate the elemental depletion in the interstellar medium (ISM) to successfully and accurately simulate the chemical evolution in various astrophysical environments. A pioneering work on elemental depletion in the ISM was presented by Jenkins,[1] who conducted a comprehensive analysis of 17 different elements. His study analyzes observational data collected from 243 sight lines in the local region of our galaxy and indicates a depletion of nearly all elements as the density of the clouds increases. The majority of the depleted elements can be found in the gas phase (molecular form) and in icy grain mantles. However, the process of sulfur depletion in dense cores has remained an unanswered question for decades, with nearly 99% of depleted sulfur still unaccounted for (see, for instance, Ref. [2] for the most recent summary of the problem). This is known as sulfur depletion or the missing sulfur problem in dark clouds or star-forming regions.[3–5] In the diffuse ISM, the gas-phase sulfur abundance is known to be in the order of a few 10^{-5} in various directions (see, for example, Refs. [5,6]). This suggests that sulfur is not depleted in the diffuse medium, as its observed abundance is similar to the cosmic sulfur abundance, which is $\sim 1.5 \times 10^{-5}$.[4] However, in dark clouds and star-forming regions, the sum of the observed abundances of sulfur species is less than 1% of the cosmic abundance.[2,3]

Current chemical models show that gas-phase sulfur species cannot fully account for sulfur's cosmic abundance. According to these results, the missing or undetected sulfur in the gas phase might exist mostly as ice on dust grains, as neutral atomic sulfur in the gas phase (see, for example, Refs. [3,4]), or as a refractory material.[2] However, SO_2 and OCS are the only S-bearing species observed in the solid phase so far.[7–9] These observational results highlight potential limitations in current chemical models. Moreover, a recent study[10] on the formation of cyanopolyynes showed that a C/O ratio of 1.1 is required to explain their observed abundance in TMC-1. Recent studies[3,4,11] on sulfur species in dark clouds have used a C/O ratio of 0.7 or lower to account for sulfur depletion. These studies, however, do not address the problem of sulfur depletion when the C/O ratio is close to 1. Herein, we present radio observations of carbon chain S-bearing species (C_2S and C_3S) in TMC-1. In addition, we use our time-dependent chemical model to explain the observed abundances and demonstrate the pivotal role of the C/O ratio in determining the extent of sulfur depletion in dense cores.

*Corresponding authors. Email: wasim@xao.ac.cn; xiaohu.li@xao.ac.cn

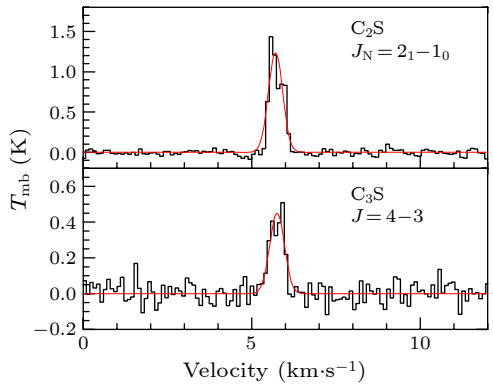

Fig. 1. The detected lines for C_2S and C_3S. The black line shows the observed spectral sequence, while the red line represents the Gaussian fitting. The corresponding molecule's name and rotational transition appear in the upper right corner.

The observations were carried out using the NSRT-26m radio telescope at the Xinjiang Astronomical Observatory, Chinese Academy of Sciences, during July 2020. The adopted coordinates for our observations were RA (J2000) = 04 : 41 : 45.9, Dec (J2000) = 25 : 41 : 27.0. We observed the rotational transition spectral lines of C_2S ($J_N = 2_1 - 1_0$) and C_3S ($J = 4 - 3$). The observed lines are listed in Table 1, and the parameters of the transitions are taken from the molecular database Splatalogue.[12] In the observation process, the typical system temperature is about 40 K. The receiver's back end uses a Digital Filter Bank with 8192 channels and a bandwidth of 64 MHz, which corresponds to a frequency resolution of 7.8125 kHz and a velocity resolution of 0.102 km·s^{-1} at 23 GHz. The half-power beam widths (HPBWs) were 100″ and 110″ for 24.2 GHz and 22 GHz, respectively. The antenna temperature (T_a^*) is related to the main beam brightness temperature (T_{mb}) via the main beam efficiency (η), i.e. $T_{mb} = T_a^*/\eta$; the value of η is $\sim$0.6. The observation adopts the position-switching mode method, and the integration times of on-source and off-source were three minutes per scan. The integration time for each molecule was one hour, including telescope overhead for position switching. The data were reduced using the GILDAS[13] software package, including CLASS and GREG. For all the observed spectral lines, we first subtract the linear baseline, and then fit these spectral lines with Gaussian fitting.

The frequency coverage on the K-band for NSRT-26m is from 22 GHz to 24.2 GHz. In this frequency range, we observed HC_5N, HC_7N, NH_3, C_2S, and C_3S in TMC-1, which is consistent with the observations reported in Ref. [14]. In this work, we are only interested in the sulfur chemistry in TMC-1.

The observed spectral lines were identified based on the molecular database Splatalogue. The centroid velocity of 5.83 km·s^{-1} for TMC-1 is adopted to derive the rest frequency of the observed lines.[15] The molecular line width in TMC-1 is usually very narrow, about 0.5 km·s^{-1}. Our observations confirm previous observations of C_2S ($J_N = 2_1 - 1_0$) and C_3S ($J = 4 - 3$) in TMC-1.[14,16] For all the identified lines, the Gaussian fitting routine in CLASS is used to derive line parameters, including the main beam brightness temperature (T_{mb}), the full width at half maximum (FWHM), the integrated intensity ($W = \int T_{mb} dv$), and the centroid velocity (V_{LSR}), which are summarized in Table 1. The observed spectral lines are shown in Fig. 1. The error of $\int T_{mb} dv$ was calculated as $\sigma_w = \sqrt{(\text{calc} \times W)^2 + [\text{rms} \times \sqrt{2 \times \text{FWHM} \times \Delta V}]^2}$. Here, calc denotes the calibration uncertainty (%) and the valve of the NSRT-26m is 14%;[17] ΔV is the velocity resolution in units of km·s^{-1}, and the rms is obtained from the statistics in regions free of obvious spectral lines.

By assuming local-thermodynamic-equilibrium conditions and assuming that lines are optically thin, the column density of species is derived by using the equation[18,19]

$$N = \frac{3k}{8\pi^3 \nu} \frac{Q(T_{ex})}{S\mu^2} \frac{e^{E_u/kT_{ex}} J_\nu(T_{ex})}{J_\nu(T_{ex}) - J_\nu(T_{bg})} \int T_{mb} dv, \quad (1)$$

where S, μ, E_u, and ν represent the intrinsic line strength, dipole moment, upper level energy, and rest frequency of the line. $Q(T_{ex})$ stands for the partition function and it was estimated as $kT_{ex}/(hB)\exp(hB/3kT_{ex})$ with B bing the rigid rotor rotation constant,[18] k the Boltzmann constant, and h the Planck constant. S, μ, B, and E_u are taken from the molecular database Splatalogue, as listed in Table 1. $J_\nu(T)$ is the equivalent Rayleigh–Jeans temperature defined by $J_\nu(T) = (h\nu/k)[\exp(h\nu/kT) - 1]^{-1}$. In these equations, T_{ex} and T_{bg} (2.73 K) represent the excitation temperature and the cosmic background temperature, and T_{mb} is the main beam brightness temperature.

Table 1. Spectral line parameters of molecules detected in TMC-1 and telescope parameters.

Molecule	Transition	ν (MHz)	μ (Debye)	S_{ij}	B (MHz)	E_u (K)	HPBW (″)	V_{chan} (m·s^{-1})	rms (mK)	$\int T_{mb} dv$ (K·km·s^{-1})	V_{LSR} (km·s^{-1})	FWHM (km·s^{-1})	T_{mb} (K)
C_2S	$J_N = 2_1 - 1_0$	22344.0300	2.81	1.982	6477.75	1.60598	109	104.8	33.94	0.661(0.093)	5.708(0.004)	0.501(0.009)	1.239
C_3S	$J = 4 - 3$	23122.9834	3.70	4.000	2890.38	2.77441	105	101.3	50.36	0.253(0.039)	5.755(0.018)	0.521(0.038)	0.453

Note: Except for $\int T_{mb} dv$, the values in parentheses are the errors of Gaussian fitting.

The column densities of these molecules have been calculated using Eq. (1), assuming an excitation temperature of 10 K. In addition, we have computed the fractional abundance of the molecules based on the column density of H_2 in TMC-1 (0.5–3.3 $\times 10^{22}$ cm^{-2} in Ref. [20]). All these results are listed in Table 2.

We used a three-phase version of the Nautilus gas-grain chemical code[21] to carry out the time-dependent simulations, in which we simulated the source as a single point and did not consider any spatial distribution of physical parameters. The time-dependent model we utilize has been thoroughly explained in Ref. [22], so we will not elaborate on it here. Our gas-phase chemistry is mostly based on the kida.uva.2016 public network with updated reactions from the KIDA[23] database. In our model, the initial abundances (with respect to H_2) of all gas and grain

species are shown in Table 3, the abundance of C^+ varies with the model according to the C/O ratio, and we also vary the abundance of S^+ to find the best fit model.

Table 2. Column density (and abundance) of molecules detected in TMC-1.

Molecule	N (cm^{-2})	$N(X)/N(H_2)$
C_2S	(1.36–1.80) $\times10^{13}$	(0.48–3.15) $\times10^{-9}$
C_3S	(3.52–4.80) $\times10^{12}$	(1.26–8.33) $\times10^{-10}$

Table 3. Elemental abundances and initial abundances.

Element	Abundance relative to H	References
H_2	0.5	
He	0.09	[24]
N	6.2×10^{-5}	[1]
O	2.4×10^{-4}	[25]
C^+	1.2×10^{-4}–2.4×10^{-4}	
S^+	8×10^{-8}–1.5×10^{-5}	
Si^+	8.0×10^{-9}	[26]
Fe^+	3.0×10^{-9}	[26]
Na^+	2.0×10^{-9}	[26]
Mg^+	7.0×10^{-9}	[26]
P^+	2.0×10^{-10}	[26]
Cl^+	1.0×10^{-9}	[26]
Ice	0	
All other gas species	0	

We present the time evolution of C_2S and C_3S abundances in the gas phase, together with NSRT observation results, in Fig. 2.

In all the models shown in Fig. 2, the major formation reactions for C_2S are

$$C_3S^+ + e^- \rightarrow C + C_2S, \quad (2)$$

$$HC_3S^+ + e^- \rightarrow CH + C_2S, \quad (3)$$

and the major destruction reactions are

$$C_2S + C^+ \rightarrow S + C_3^+, \quad (4)$$

$$C_2S + C^+ \rightarrow C + C_2S^+, \quad (5)$$

$$C_2S + O \rightarrow CO + CS. \quad (6)$$

Here we can see that C^+ and O are major causes of C_2S destruction and play a key role in determining the gas-phase abundance of C_2S. For example, in Fig. 2, at time 2×10^3 yr, we note a sharp drop in the gas-phase abundance of C_2S. On inspection, we can find that at this point in the simulation there is a sharp decrease in the abundance of C^+, which makes more O available for the destruction of C_2S. As a result, $C_2S + O \rightarrow CO + CS$ becomes the major destruction reaction and controls the gas-phase abundance of C_2S.

Again, in all our simulations, the major formation reactions for C_3S are

$$C_4S^+ + e^- \rightarrow C + C_3S, \quad (7)$$

$$HC_3S^+ + e^- \rightarrow H + C_3S, \quad (8)$$

$$HC_4S^+ + e^- \rightarrow CH + C_3S, \quad (9)$$

and the major destruction reactions are

$$C_3S + C^+ \rightarrow S + C_4^+, \quad (10)$$

$$C_3S + C^+ \rightarrow C + C_3S^+, \quad (11)$$

$$C_3S + H_3^+ \rightarrow H_2 + HC_3S^+. \quad (12)$$

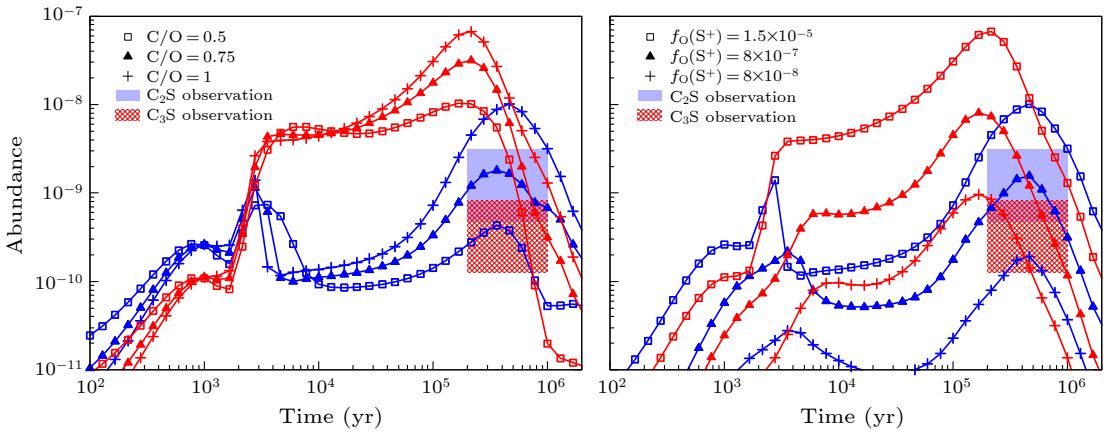

Fig. 2. Left: Impact of varying C/O ratio on the simulated gas-phase abundances of C_2S (blue lines) and C_3S (red lines) with respect to H_2, with $f_O(S^+) = 1.5\times10^{-5}$. Right: Impact of sulfur depletion on the simulated abundance of C_2S (blue lines) and C_3S (red lines), with C/O = 1. Simulated abundance values are compared with observed values within the time range from 2×10^5 yr to 10^6 yr, which are the lower and upper limits for the suggested age of the TMC-1 cloud.[4,11]

We can see that the case of C_3S is different from C_2S because its destruction rate by O is negligible. The gas-phase abundance of C_3S increases with evolution time and does not fall at time 2×10^3 yr when we have excess O in the gas phase. The abundance of C_3S decreases only when the abundance of H_3^+ becomes significant after 10^5 yr in simulation and the $C_3S + H_3^+ \rightarrow H_2 + HC_3S^+$ reaction becomes the major controlling factor of C_3S abundance in the gas phase.

In the left panel of Fig. 2, we plot the variation in simu-

lated abundances of C_2S and C_3S for different C/O ratios, with the initial sulfur abundance $[f_O(S^+)]$ kept constant at its cosmic value of 1.5×10^{-5}. From this plot, it is evident that simulation results can explain the observed abundances when the C/O ratio is 0.75, without accounting for depleted sulfur abundance. In the right panel in Fig. 2, we show that when C/O = 1, a depleted sulfur abundance $[f_O(S^+) = 8 \times 10^{-7}]$ is necessary to reproduce the observed abundances. Previous studies on sulfur species in TMC-1, such as Refs. [3,4] and the best fit model in Ref. [11], used C/O = 0.36, 0.7, and 0.5, respectively, all of which are significantly lower values than C/O = 1.1, which is required to explain the observations of cyanopolyynes in TMC-1.[10]

In our simulation results, C_2S and C_3S together account for about 0.5–1% of sulfur depletion, depending on simulation time. Since our simulation results can explain the observed abundance of C_2S and C_3S, we can say that detected C_2S and C_3S can explain about 1% of sulfur depletion in dense cores such as TMC-1. Despite the fact that C_2S and C_3S contribute to a small fraction of elemental sulfur depletion in dense cores, their gas-phase abundances strongly depend on initial sulfur abundance and C/O ratio. Due to the limitations of NSRT, other S-bearing species could not be detected. However, our simulations show similar results for other S-bearing species such as CS, C_4S, OCS, SO, SO_2, HS, H_2S, and H_2CS. Hence, the major conclusion of our finding that C/O ratio plays a key role in determining sulfur depletion in dense cores, such as TMC-1, is likely to remain true when more S-bearing species are included in future work.

Due to poor constraints on the C/O ratio in dense cores,[3,4,10,11] calculating the elemental depletion of sulfur through chemical simulation is a challenging task. Nevertheless, using currently available reaction networks[4] our simulation results suggest that depending on the type of dense core, determined by the C/O ratio, sulfur depletion could occur in sources where the C/O ratio exceeds 0.75. Our results indicate that C/O ratio is a crucial parameter, and plays a key role in determining the evolution of S-bearing species. Therefore, the C/O ratio should be chosen carefully based on the source type; otherwise, it could result in significant inaccuracies in the simulation results. Furthermore, better observational constraints on the exact C/O ratio are required for successful astronomical simulations of C_2S and C_3S abundances, as well as the abundances of other S-bearing species.

In recent years, the Chinese Five-Hundred-Meter Aperture Spherical Radio Telescope (FAST) has made significant progress in various fields of astronomy due to its super-high sensitivity. TMC-1, one of the most well-known "molecular factories" in space, is an ideal target for FAST to seek new (including, but not limited to, S-bearing) species in space. Progress in astrochemical models will play a greater and more critical role in explaining and predicting the observations.

Acknowledgements. This work was supported by the Natural Science Foundation of Xinjiang Uygur Autonomous Region (Grant No. 2022D01B221). C.L. Yang, T. Yang, Y. Zhang, and X. Fang thank the Xinjiang Tianchi Talent Program (2023). We wish to thank the NSRT operators for their assistance during the observations. The Nanshan-26m Radio Telescope is partly supported by the Operation, Maintenance and Upgrading Fund for Astronomical Telescopes and Facility Instruments, budgeted from the Ministry of Finance of China and administrated by the Chinese Academy of Sciences, and the Urumqi Nanshan Astronomy and Deep Space Exploration Observation and Research Station of Xinjiang (Grant No. XJYWZ2303).

References

[1] Jenkins E B 2009 arXiv:0905.3173 [astro-ph.GA]
[2] Rocha C M R, Roncero O, Bulut N, Zuchowski P, Navarro-Almaida D, Fuente A, Wakelam V, Loison J C, Roueff E, Goicoechea J R, Esplugues G, Beitia-Antero L, Caselli P, Lattanzi V, Pineda J, Le G R, Rodríguez-Baras M, and Riviere-Marichalar P 2023 arXiv:2307.00311 [astro-ph.GA]
[3] Laas J C and Caselli P 2019 arXiv:1903.01232 [astro-ph.GA]
[4] Vidal T H G, Loison J C, Jaziri A Y, Ruaud M, Gratier P, and Wakelam V 2017 arXiv:1704.01404 [astro-ph.GA]
[5] Howk J C, Sembach K R, and Savage B D 2006 arXiv:astro-ph/0508470 [astro-ph]
[6] Neufeld D A, Godard B, Gerin M, Pineau D F G, Bernier C, Falgarone E, Graf U U, Güsten R, Herbst E, Lesaffre P, Schilke P, Sonnentrucker P, and Wiesemeyer H 2015 arXiv:1502.05710 [astro-ph.GA]
[7] Palumbo M E, Tielens A G G M, and Tokunaga A T 1995 *Astrophys. J.* **449** 674
[8] Boogert A C A, Schutte W A, Helmich F P, Tielens A G G M, and Wooden D H 1997 *Astron. Astrophys.* **317** 929
[9] Ferrante R F, Moore M H, Spiliotis M M, and Hudson R L 2008 *Astrophys. J.* **684** 1210
[10] Loomis R A, Burkhardt A M, Shingledecker C N, Charnley S B, Cordiner M A, Herbst E, Kalenskii S, Lee K L K, Willis E R, Xue C, Remijan A J, McCarthy M C, and McGuire B A 2021 arXiv:2009.11900 [astro-ph.GA]
[11] Chen L F, Li D, Quan D, Zhang X, Chang Q, Li X, and Xiao L 2022 arXiv:2203.00174 [astro-ph.GA]
[12] https://splatalogue.online/advanced.php
[13] https://www.iram.fr/IRAMFR/GILDAS
[14] Kaifu N, Ohishi M, Kawaguchi K, Saito S, Yamamoto S, Miyaji T, Miyazawa K, Ishikawa S I, Noumaru C, Harasawa S, Okuda M, and Suzuki H 2004 *Publ. Astron. Soc. Jpn.* **56** 69
[15] Cernicharo J, Marcelino N, Agúndez M, Bermúdez C, Cabezas C, Tercero B, and Pardo J R 2020 arXiv:2009.07686 [astro-ph.GA]
[16] Suzuki H, Yamamoto S, Ohishi M, Kaifu N, Ishikawa S I, Hirahara Y, and Takano S 1992 *Astrophys. J.* **392** 551
[17] Wu G, Qiu K, Esimbek J, Zheng X, Henkel C, Li D, and Han X 2018 arXiv:1805.11242 [astro-ph.GA]
[18] Mangum J G and Shirley Y L 2015 arXiv:1501.01703 [astro-ph.IM]
[19] Caselli P, Walmsley C M, Zucconi A, Tafalla M, Dore L, and Myers P C 2002 arXiv:astro-ph/0109023 [astro-ph]
[20] Fehér O, Tóth L V, Ward-Thompson D, Kirk J, Kraus A, Pelkonen V M, Pintér S, and Zahorecz S 2016 arXiv:1603.05844 [astro-ph.GA]
[21] Ruaud M, Wakelam V, and Hersant F 2016 arXiv:1604.05216 [astro-ph.GA]
[22] Mondal S K, Iqbal W, Gorai P, Bhat B, Wakelam V, and Das A 2022 arXiv:2211.03066 [astro-ph.GA]
[23] https://kida.astrochem-tools.org/
[24] Wakelam V and Herbst E 2008 arXiv:0802.3757 [astro-ph]
[25] Hincelin U, Wakelam V, Hersant F, Guilloteau S, Loison J C, Honvault P, and Troe J 2011 arXiv:1104.1530 [astro-ph.SR]
[26] Graedel T E, Langer W D, and Frerking M A 1982 *Astrophys. J. Suppl. Ser.* **48** 321